ISSN 1392 - 1207. MECHANIKA. 2011. 17(1): 30-37

Analytical solution for thermal stresses of laminated hollow cylinders under transient nonuniform thermal loading

M. A. Ehteram*, M. Sadighi, H. Basirat Tabrizi*****
**Amirkabir University of Technology, 424 Hafez Avenue, Tehran 15875-4413, Iran, E-mail: ali_ehteram@aut.ac.ir*
***Amirkabir University of Technology, 424 Hafez Avenue, Tehran 15875-4413, Iran, E-mail: mojtaba@aut.ac.ir*
****Amirkabir University of Technology, 424 Hafez Avenue, Tehran 15875-4413, Iran, E-mail: hbasirat@aut.ac.ir*

crossref http://dx.doi.org/10.5755/j01.mech.17.1.200

1. Introduction

Filament-wound composite pipes and vessels are widely used in commercial industries such as fuel tanks, portable oxygen storage, and compressed natural gas (CNG) pressure vessel transportation. Using of these materials under a high temperature environment is increasing. One of the causes for damage in these laminated composite materials includes delimitation. In order to evaluate this phenomenon, the thermal stress analysis taking into account the transverse shearing stresses and the normal stress in the thickness direction is necessary. In addition, a transient thermal stress analysis as well as a steady thermal stress analysis becomes important, because maximum thermal stress distribution occurs in a transient state.

Lee [1] preformed the analysis of thermal stresses within multilayered cylinder under axial symmetry periodic boundary conditions. Ootao and Tanigawa [2] considered an angle-ply laminated cylindrical panel with simply supported edges due to a nonuniform heat supply in the circumferential direction. Shahani and Nabavi [3] solved transiented thermoelasticity problem in an isotropic thick-walled cylinder analytically by using the finite Hankel transform. Talor and Radu [4] considered the sinusoidal transient temperature for an isotropic hollow cylinder in an axis symmetric condition for the analyses of the thermal fatigue in the pipe lines. Hocine [5] investigated on thermo-mechanical behaviour of multilayer tubular composite in axis metric steady state conditions. His results show that thermal effect has the greatest influence on radial stresses and strains. Zamani Nejad and Rahimi developed a complete and consistent 3-D set of field equa-tions by tensor analysis to characterize the behavior of FGM thick shells of revolution with arbi-trary curvature and variable thickness along the meridional direction [6].

Bakaiyan and Hosseini [7] studied the stress and deformation of the filament-wound pipes under combined internal pressure and temperature variations with axisymmetric and steady-state consideration.

In the previous works thermal conduction and elasticity equations was solved only for the steady or the symmetric condition.

This investigation is concerned with the theoretical treatment of the transient thermal stress problem involving a two layered anisotropic hollow cylinder with non uniform temperature in the circumferential direction.

2. Analyses

An infinitely long angle-ply laminated hollow cylinder composed of N layers is shown in Fig. 1. The cylinder's inner and outer radii are denoted as a and b respectively. It is assumed that each layer has the orthotropic material properties and the fiber direction in the ith layer is alternated with ply angle φ to the z-axis.

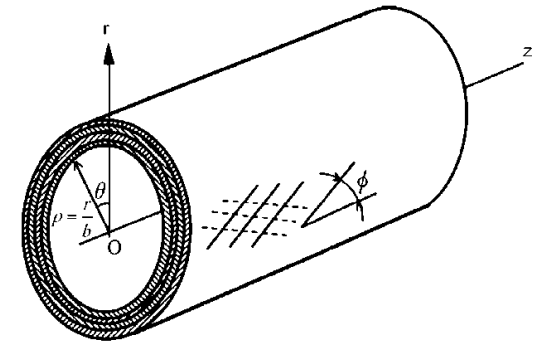

a

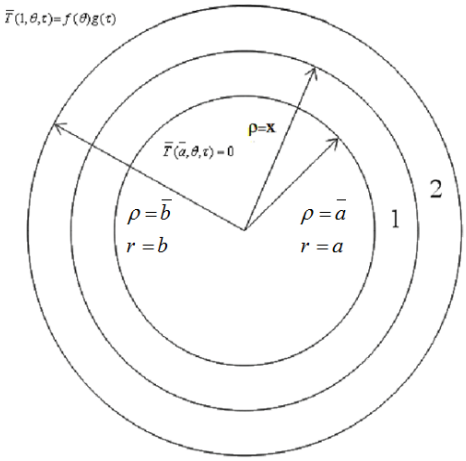

b

Fig. 1 a) Coordinate system and b) boundary conditions of a multi layered hollow cylinder with inner and outer radii are denoted as a and b respectively

2.1 Heat conduction problem

It is assumed that initially the laminated hollow cylinder is at constant temperature and the temperature of outer surface changes by an arbitrary function of time and angle of the form $\bar{f}(\theta)\bar{g}(\tau)$. The temperature distribution is assumed to be a two-dimensional distribution in r–θ plane. The transient heat conduction of each layer and the initial and thermal boundary conditions in a dimensionless form are given in the following forms [2]

$$\frac{\partial \bar{T}}{\partial \tau} = \overline{K_r}\left(\frac{\partial^2 \bar{T}}{\partial \rho^2} + \frac{\partial \bar{T}}{\rho \partial \rho}\right) + \frac{\overline{K_\theta}}{\rho^2}\frac{\partial^2 \bar{T}}{\partial \theta^2} \tag{1}$$

$$\overline{T}\Big|_{\rho=\bar{a}} = 0, \overline{T}\Big|_{\tau=0} = 0, \ \overline{T}\Big|_{\rho=1} = \overline{f}(\theta)\overline{g}(\tau) \tag{2}$$

$$\overline{T}\Big|_{\theta=0} = \overline{T}\Big|_{\theta=2\pi}, \overline{T}_{,\theta}\Big|_{\theta=0} = \overline{T}_{,\theta}\Big|_{\theta=2\pi} \tag{3}$$

where

$$\left.\begin{aligned} \overline{K_r} &= \overline{K}_T \\ \overline{K}_\theta &= \overline{K}_L \sin^2(\Phi) + \overline{K}_T \cos^2(\Phi) \end{aligned}\right\} \tag{4}$$

The following dimensionless values are introduced

$$\left.\begin{aligned} \left(\rho, R, \bar{a}\right) &= \frac{\left(r, r_i, a\right)}{b} \\ ((\overline{K_r}, \overline{K_\theta}, \overline{K_L}, \overline{K_T}) &= \frac{(K_r, K_\theta, K_L, K_T)}{K_0} \\ \tau = \frac{K_0 t}{b^2}, \overline{T} &= \frac{T - T_0}{T_0} \end{aligned}\right\} \tag{5}$$

where T is the temperature, K_r and K_θ are the thermal diffusivities in the r and θ directions, respectively, λ_r is the thermal conductivity in the r direction, t is time, T_0, K_0 and λ_0 are the typical values of temperature, thermal diffusivity and thermal conductivity, respectively. In Eq. (4) the subscripts L and T denote the fiber and transverse directions, respectively. $\overline{g}(\tau)$ and $\overline{f}(\theta)$ are the arbitrary functions of time and angle respectively. Introducing the finite sine transformation with respect to the variable θ, the solution of Eq. (1) can be obtained to satisfy Eq. (3). This solution is shown as follows

$$\overline{T} = \overline{K_r}\frac{2\bar{a}}{\pi}\sum_{n=1}^{\infty}\sum_{j=1}^{\infty} a_j [Kernel(\rho, \lambda_j)] \frac{\int_0^\tau \overline{g}(t) e^{\overline{Kr}.\lambda_j^2.t} dt (A_n \sin(n\theta) + B_n \cos(n\theta))}{\pi e^{\overline{Kr}.\lambda_j^2 \tau}} \tag{10}$$

where

$$\left.\begin{aligned} A_n &= \int_{-\pi}^{\pi} f(\theta)\sin(n\theta)d\theta \\ B_n &= \int_{-\pi}^{\pi} f(\theta)\cos(n\theta)d\theta \\ a_j &= \frac{1}{\int_a^1 \rho\,[Kernel(\rho, \lambda_j)]^2 d\rho} \\ Kernel(\rho, \lambda_j) &= \\ &= Y_\eta(\lambda_j) J_\eta(\lambda_j \rho) - J_\eta(\lambda_j) Y_\eta(\lambda_j \rho) \end{aligned}\right\} \tag{11}$$

and λ_j are the positive roots of $Kernel(\bar{a}, \lambda_j) = 0$. Also from [7]

$$\begin{aligned} &\int_a^1 \rho\,[Kernel(\rho, \lambda_j)]^2 d\rho = \\ &= 5(J_\eta^2(\lambda_j)[\overline{A}(1) - \bar{a}^2 \overline{A}(\bar{a})] - \\ &-2J_\eta(\lambda_j).Y_\eta(\lambda_j)[\overline{B}(1) - \bar{a}^2 \overline{B}(\bar{a})] + \\ &+Y_\eta(\lambda_j)^2[\overline{C}(1) - \bar{a}^2 \overline{C}(\bar{a})]) \end{aligned} \tag{12}$$

where

$$\overline{T} = \sum_{n=1}^{\infty} \overline{T_n}(\rho, \tau)(C_1 \sin(n\theta) + C_2 \cos(n\theta)) \tag{6}$$

where C_1 and C_2 are constants and can be found from Eq. (2). By using Fourier transform for function $\overline{f}(\theta)$, Eq. (2) can be written as

$$\begin{aligned} \overline{f}(\theta) &= \sum_{n=1}^{\infty} (A_n \sin(n\theta) + B_n \cos(n\theta))\overline{g}(\tau) = \\ &= \sum_{n=1}^{\infty} \overline{T}_n(1, \tau)(C_1 \sin(n\theta) + C_2 \cos(n\theta)) \end{aligned} \tag{7}$$

As a result, it is obvious that

$$C_1 = A_n, C_2 = B_n, \overline{T_n}(1, \tau) = \overline{g}(\tau) \tag{8}$$

Since, the function $\overline{T_n}(\rho, \tau)$ is still unknown, accordingly, substituting $\overline{T}$ from Eq. (6) into Eq. (1) results in

$$\frac{1}{\overline{K_r}}\frac{\partial \overline{T_n}(\rho, \tau)}{\partial \tau} = \frac{\partial\left(\rho \dfrac{\overline{T_n}(\rho, \tau)}{\partial \rho}\right)}{\rho\,\partial\rho} + \frac{\overline{K_\theta}}{\overline{K_r}}\frac{n^2}{\rho^2}\overline{T_n}(\rho, \tau) \tag{9}$$

The solution of the Eq. (9) may be accomplished by using the finite Hankel transform as described in [8].

Finally, the temperature distribution in the cylinder can be written as

$$\left.\begin{aligned} \overline{A}(x) &= J_\eta^2(\lambda_j x) - J_{\eta-1}(\lambda_j x) J_{\eta+1}(\lambda_j x) \\ \overline{C}(x) &= Y_\eta^2(\lambda_j x) - Y_{\eta-1}(\lambda_j x) Y_{\eta+1}(\lambda_j x) \\ \overline{B}(x) &= 5(2J_\eta(\lambda_j x) Y_\eta(\lambda_j x) - \\ &- J_{\eta+1}(\lambda_j x) Y_{\eta-1}(\lambda_j x) - J_{\eta-1}(\lambda_j x) Y_{\eta+1}(\lambda_j x)) \end{aligned}\right\}. \tag{13}$$

2.2. Thermal stress analyses

In this section, the transient thermal stress of a laminated hollow cylinder is analyzed as a generalized plane strain problem. In each layer, the fiber direction, the in-plane transverse direction and the radial direction are denoted by L, T and R, respectively. Each layer has orthotropic material properties between the fiber-reinforced direction and its orthogonal direction.

$$\begin{Bmatrix} \overline{\sigma}_{LL} \\ \overline{\sigma}_{TT} \\ \overline{\sigma}_{RR} \\ \overline{\sigma}_{TR} \\ \overline{\sigma}_{RL} \\ \overline{\sigma}_{LT} \end{Bmatrix} = \begin{bmatrix} \overline{Q}_{11} & \overline{Q}_{12} & \overline{Q}_{12} & 0 & 0 & 0 \\ \overline{Q}_{12} & \overline{Q}_{22} & \overline{Q}_{23} & 0 & 0 & 0 \\ \overline{Q}_{12} & \overline{Q}_{23} & \overline{Q}_{22} & 0 & 0 & 0 \\ 0 & 0 & 0 & \overline{Q}_{44} & 0 & 0 \\ 0 & 0 & 0 & 0 & \overline{Q}_{55} & 0 \\ 0 & 0 & 0 & 0 & 0 & \overline{Q}_{66} \end{bmatrix} \begin{Bmatrix} \overline{\varepsilon}_{LL} - \overline{\alpha}_L \overline{T} \\ \overline{\varepsilon}_{TT} - \overline{\alpha}_T \overline{T} \\ \overline{\varepsilon}_{RR} - \overline{\alpha}_T \overline{T} \\ \overline{\gamma}_{r\theta} \\ \overline{\gamma}_{rz} \\ \overline{\gamma}_{\theta z} - \overline{\alpha}_{\theta z} \overline{T} \end{Bmatrix} \tag{14}$$

Stress-strain relations in the dimensionless form for the *i*th layer are given in Eq. (14) .Applying the coordinate transformation rule to Eq.(14), stress-strain relations for the global coordinate system (r, θ, z) are

$$\begin{Bmatrix} \overline{\sigma}_{zz} \\ \overline{\sigma}_{\theta\theta} \\ \overline{\sigma}_{rr} \\ \overline{\sigma}_{r\theta} \\ \overline{\sigma}_{rz} \\ \overline{\sigma}_{z\theta} \end{Bmatrix} = \begin{bmatrix} \overline{Q}^*_{11} & \overline{Q}^*_{12} & \overline{Q}^*_{13} & 0 & 0 & \overline{Q}^*_{16} \\ \overline{Q}^*_{12} & \overline{Q}^*_{22} & \overline{Q}^*_{23} & 0 & 0 & \overline{Q}^*_{26} \\ \overline{Q}^*_{13} & \overline{Q}^*_{23} & \overline{Q}^*_{33} & 0 & 0 & \overline{Q}^*_{36} \\ 0 & 0 & 0 & \overline{Q}^*_{44} & \overline{Q}^*_{45} & 0 \\ 0 & 0 & 0 & \overline{Q}^*_{45} & \overline{Q}^*_{55} & 0 \\ \overline{Q}^*_{16} & \overline{Q}^*_{26} & \overline{Q}^*_{36} & 0 & 0 & \overline{Q}^*_{66} \end{bmatrix} \times$$

$$\times \begin{Bmatrix} \overline{\varepsilon}_{zz} - \overline{\alpha}_z \overline{T} \\ \overline{\varepsilon}_{\theta\theta} - \overline{\alpha}_\theta \overline{T} \\ \overline{\varepsilon}_{rr} - \overline{\alpha}_r \overline{T} \\ \overline{\gamma}_{r\theta} \\ \overline{\gamma}_{rz} \\ \overline{\gamma}_{\theta z} - \overline{\alpha}_{\theta z} \overline{T} \end{Bmatrix} \tag{15}$$

where

$$\left.\begin{aligned}
&\overline{Q}^*_{11} = m^4 \overline{Q}_{11} + 2m^2 n^2 (\overline{Q}_{12} + \overline{Q}_{66}) + n^4 \overline{Q}_{22} \\
&\overline{Q}^*_{12} = m^4 \overline{Q}_{12} + m^2 n^2 (\overline{Q}_{11} + \overline{Q}_{22} - 2\overline{Q}_{66}) + n^4 \overline{Q}_{12} \\
&\overline{Q}^*_{13} = m^2 \overline{Q}_{12} + n^2 \overline{Q}_{23} \\
&\overline{Q}^*_{16} = mn(m^2(\overline{Q}_{11} - \overline{Q}_{12} + \overline{Q}_{66}) + \\
&+n^2(\overline{Q}_{12} - \overline{Q}_{22} - \overline{Q}_{66})) \\
&\overline{Q}^*_{22} = m^4 \overline{Q}_{22} + 2m^2 n^2 (\overline{Q}_{12} + \overline{Q}_{66}) + n^4 \overline{Q}_{11} \\
&\overline{Q}^*_{23} = n^2 \overline{Q}_{12} + m^2 \overline{Q}_{23} \\
&\overline{Q}^*_{26} = mn(m^2(\overline{Q}_{12} - \overline{Q}_{22} + \overline{Q}_{66}) + \\
&+n^2(\overline{Q}_{11} - \overline{Q}_{12} - \overline{Q}_{66})) \\
&\overline{Q}^*_{36} = mn(\overline{Q}_{12} - \overline{Q}_{23}); \overline{Q}^*_{44} = \frac{(m^2 \overline{Q}_{44} + n^2 \overline{Q}_{55})}{2} \\
&\overline{Q}^*_{45} = \frac{mn(\overline{Q}_{55} - \overline{Q}_{44})}{2}; \overline{Q}^*_{55} = \frac{(n^2 \overline{Q}_{44} + m^2 \overline{Q}_{55})}{2} \\
&\overline{Q}^*_{66} = m^2 n^2 (\overline{Q}_{11} + \overline{Q}_{22} - 2\overline{Q}_{12} - \overline{Q}_{66}) + \\
&+(m^4 + n^4)\overline{Q}_{66}/2; \overline{Q}^*_{33} = \overline{Q}_{22} \\
&\overline{\alpha}_z = m^2 \overline{\alpha}_L + n^2 \overline{\alpha}_T, \overline{\alpha}_\theta = n^2 \overline{\alpha}_L + m^2 \overline{\alpha}_T \\
&\overline{\alpha}_z = \overline{\alpha}_T \; \overline{\alpha}_{\theta z} = 2mn(\overline{\alpha}_L - \overline{\alpha}_T) \\
&m = cos\phi, n = sin\phi
\end{aligned}\right\} \tag{16}$$

In the above equations, the following dimensionless values are introduced

$$\left.\begin{aligned}
&\overline{\sigma}_{kl} = \frac{\sigma_{kl}}{\alpha_0 E_0 T_0}, (\overline{\varepsilon}_{kl}, \overline{\gamma}_{kl}) = \frac{(\varepsilon_{kl}, \gamma_{kl})}{\alpha_0 T_0} \\
&(\overline{\alpha}_{kl}, \overline{\alpha}_{\theta z}) = \frac{(\alpha_{kl}, \alpha_{\theta z})}{\alpha_0}, (\overline{Q}_{kl}, \overline{Q}_{kl}) = \frac{(Q_{kl}, Q_{kl})}{E_0} \\
&(\overline{u}_r, \overline{u}_\theta, \overline{u}_z) = (u_r, u_\theta, u_z)/\alpha_0 T_0 b
\end{aligned}\right\} \tag{17}$$

where σ_{kli} are the stress components, ε_{kli} are the strain tensor, α_{ki} and $\alpha_{\theta zi}$ are the coefficients of linear thermal expansion, Q_{kli} and Q^*_{kli} are the elastic stiffness constants, and $\alpha_0 = \alpha_r$ and $E_0 = E_r$ are the typical values of the coefficient of linear thermal expansion and Young's modulus of elasticity, respectively. The strain-displacement equations can be displayed as flowing equations

$$\left.\begin{aligned}
&\overline{\varepsilon}_r = \overline{u}_{r,\rho}, \overline{\varepsilon}_\theta = \frac{1}{\rho}\overline{u}_{\theta,\theta} + \frac{\overline{u}_r}{\rho}, \overline{\varepsilon}_z = \frac{\partial \overline{u}_z}{\partial z} \\
&2\overline{\varepsilon}_{r\theta} = \left(\frac{\overline{u}_{r,\theta}}{\rho} + \overline{u}_{\theta,\rho} - \frac{\overline{u}_\theta}{\rho}\right), 2\overline{\varepsilon}_{rz} = \overline{u}_{p,z} + \overline{u}_{z,\rho} \\
&2\overline{\varepsilon}_{z\theta} = \overline{u}_{\theta,z} + \frac{\overline{u}_{z,\theta}}{\rho}
\end{aligned}\right\} \tag{18}$$

Using stress - strain Eqs. (18), the displacement equations can be displayed in the following form

$$\left.\begin{aligned}
&\overline{Q_{33}}^*\left(\overline{u}_{r,\rho\rho} + \rho^{-1}\overline{u}_{r,\rho}\right) - \rho^{-2}\left(\overline{Q_{22}}^*\overline{u}_r - \overline{Q_{44}}^*\overline{u}_{r,\theta\theta}\right) + \\
&+\left(\overline{Q_{23}}^* + \overline{Q_{44}}^*\right)\rho^{-1}\overline{u}_{\theta,\rho\theta} - \left(\overline{Q_{22}}^* + \overline{Q_{44}}^*\right)\rho^{-2}\overline{u}_{\theta,\theta} + \\
&+\left(\overline{Q_{36}}^* + \overline{Q_{45}}^*\right)\rho^{-1}\overline{u}_{z,\rho\theta} - \overline{Q_{26}}^*\rho^{-2}\overline{u}_{z,\theta} = \\
&= \overline{\beta}_r \overline{T}_{,\rho} + \left(\overline{\beta}_r - \overline{\beta}_\theta\right)\rho^{-1}\overline{T} \\
&\rho^{-1}\left(\overline{Q_{44}}^* + \overline{Q_{23}}^*\right)\left(\overline{u}_{r,\rho\theta}\right) + \rho^{-2}\left(\overline{Q_{44}}^* + \overline{Q_{22}}^*\right)\overline{u}_{r,\theta} + \\
&+\overline{Q_{44}}^*\left(\rho^{-1}\overline{u}_{\theta,\rho} - \rho^{-2}\overline{u}_\theta + \overline{u}_{\theta,\rho\rho}\right) + \\
&+\overline{Q_{22}}^*\rho^{-2}\overline{u}_{\theta,\theta\theta} + \overline{Q_{45}}^*\left(2\rho^{-1}\overline{u}_{z,\rho} + \overline{u}_{z,\rho\rho}\right) + \\
&+\overline{Q_{26}}^*\rho^{-2}\overline{u}_{z,\theta\theta} = \overline{\beta}_\theta \rho^{-1}\overline{T}_{,\theta} \\
&\rho^{-1}\left(\overline{Q_{36}}^* + \overline{Q_{45}}^*\right)\left(\overline{u}_{r,\rho\theta}\right) + \rho^{-2}\overline{Q_{26}}^*\overline{u}_{r,\theta} + \overline{Q_{45}}^*\overline{u}_{\theta,\rho\rho} + \\
&+\overline{Q_{26}}^*\rho^{-2}\overline{u}_{\theta,\theta\theta} + \overline{Q_{55}}^*\left(\rho^{-1}\overline{u}_{z,\rho} + \overline{u}_{z,\rho\rho}\right) + \\
&+\overline{Q_{66}}^*\rho^{-2}\overline{u}_{z,\theta\theta} = \overline{\beta}_{\theta z}\rho^{-1}\overline{T}_{,\theta}
\end{aligned}\right\} \tag{19}$$

where

$$\begin{bmatrix} \overline{\beta}_z \\ \overline{\beta}_\theta \\ \overline{\beta}_r \\ \overline{\beta}_{\theta z} \end{bmatrix} = \begin{bmatrix} \overline{Q_{11}}^* & \overline{Q_{12}}^* & \overline{Q_{13}}^* & \overline{Q_{16}}^* \\ \overline{Q_{12}}^* & \overline{Q_{22}}^* & \overline{Q_{23}}^* & \overline{Q_{26}}^* \\ \overline{Q_{13}}^* & \overline{Q_{32}}^* & \overline{Q_{33}}^* & \overline{Q_{36}}^* \\ \overline{Q_{16}}^* & \overline{Q_{26}}^* & \overline{Q_{36}}^* & \overline{Q_{66}}^* \end{bmatrix} \begin{bmatrix} \overline{\alpha_z} \\ \overline{\alpha_\theta} \\ \overline{\alpha_r} \\ \overline{\alpha_{\theta z}} \end{bmatrix} \tag{20}$$

In the above equations, comma denotes partial differentiation with respect to variables that follows. The boundary conditions in the surface and interfaces are represented accordingly

$$\left.\begin{aligned}
&\rho = \overline{a} : \overline{\sigma}_{rr} = 0, \overline{\sigma}_{r\theta} = 0, \overline{\sigma}_{rz} = 0 \\
&\rho = 1 : \overline{\sigma}_{rr} = 0, \overline{\sigma}_{r\theta} = 0, \overline{\sigma}_{rz} = 0 \\
&\rho = r_i : \overline{\sigma}_{rr,i} = \overline{\sigma}_{rr,i+1}, \overline{\sigma}_{r\theta,i} = \overline{\sigma}_{r\theta,i+1} \\
&\overline{\sigma}_{rz,i} = \overline{\sigma}_{rz,i+1}, \overline{u}_{r,i} = \overline{u}_{r,i+1} \\
&\overline{u}_{\theta,i} = \overline{u}_{\theta,i+1}, \overline{u}_{z,i} = \overline{u}_{z,i+1}
\end{aligned}\right\} \tag{21}$$

Here, we deal with nonuniform thermal loading. However, mechanical loading can be considered with equality of radial stresses with this kind of loading in the boundary conditions.

2.3 Solving equations

In order to satisfy periodic condition in the angular direction, the solutions of Eq. (14) are assumed in the following form

$$\left.\begin{aligned}&\bar{u}_k=\sum_{n=1}^{\infty}(U_{kn}(\rho))(A_n sin(n\theta)+B_n cos(n\theta))\\&K=r,\theta,z\end{aligned}\right\} \tag{22}$$

Substituting Eq. (22) into Eq. (19) and considering $\rho=e^s$ for the left hand side of Eq. (19), it can be written as

$$\left.\begin{aligned}&\left[\overline{Q_{33}}^*\left(\overline{D}^2\right)-\left(\overline{Q_{22}}^*+n^2\overline{Q_{44}}^*\right)\right]U_{rn}-\left[n\left(\overline{Q_{23}}^*+\overline{Q_{44}}^*\right)\overline{D}-n\left(\overline{Q_{22}}^*+\overline{Q_{44}}^*\right)\right]U_{\theta n}-n\left[\left(\overline{Q_{36}}^*+\overline{Q_{45}}^*\right)\overline{D}-\overline{Q_{26}}^*\right]U_{zn}=\\&=\overline{\beta}_r\overline{T}\rho\tau n_{,\rho}+\left(\overline{\beta}_r-\overline{\beta}_\theta\right)\rho^{-1}\overline{T}\rho\tau n\\&\left[\left(\overline{Q_{44}}^*+\overline{Q_{23}}^*\right)\overline{D}+\left(\overline{Q_{44}}^*+\overline{Q_{22}}^*\right)\right]n\left(U_{rn}\right)+\left[\overline{Q_{44}}^*\overline{D}^2-\left(\overline{Q_{44}}^*+\overline{Q_{22}}^*n^2\right)\right]U_{\theta n}+\\&+\left[\left(\overline{Q_{45}}^*\right)\overline{D}\left(\overline{D}+1\right)-n^2.\overline{Q_{26}}^*\right]U_{zn}=n\overline{\beta}_\theta\rho^{-1}\overline{T}\rho\tau n\\&n\left[\left(\overline{Q_{36}}^*+\overline{Q_{45}}^*\right)\overline{D}+\overline{Q_{26}}^*\right]U_{rn}+\left[\overline{Q_{45}}^*\overline{D}\left(\overline{D}-1\right)-n^2\left(\overline{Q_{26}}^*\right)\right]U_{\theta n}+\\&+\left[\left(\overline{Q_{55}}^*\right)\overline{D}^2-n^2.\overline{Q_{66}}^*\right]U_{zn}=n\overline{\beta}_{\theta z}\rho^{-1}\overline{T}\rho\tau n\end{aligned}\right\} \tag{23}$$

where $\overline{D}=\dfrac{\partial}{\partial s}$. This is a system of the second order differential equations which can be explained as the first order equations as

$$\left.\begin{aligned}&U'_{rn}=\overline{D}U_{rn},\overline{D}^2U_{rn}=\overline{D}U'_{rn}\\&U'_{\theta n}=\overline{D}U_{\theta n},\overline{D}^2U_{\theta n}=\overline{D}U'_{\theta n}\\&U'_{zn}=\overline{D}U_{zn},\overline{D}^2U_{zn}=\overline{D}U'_{zn}\end{aligned}\right\} \tag{24}$$

Substituting Eq. (24) into Eq. (23), the system of equations can be written in a matrix form of

$$\begin{aligned}&(\overline{\overline{A}}\,\overline{D}-\overline{\overline{B}})\overline{\overline{U}}_n=\overline{\overline{M}}_T\Rightarrow\\&\Rightarrow[I\overline{D}-\overline{\overline{A}}^{-1}\overline{\overline{B}}]\overline{U_{cn}}=\overline{\overline{A}}^{-1}\overline{\overline{M}}_T\end{aligned} \tag{25}$$

The double bar notation is used for displaying matrix essence of parameters and $\overline{\overline{A}}$, $\overline{\overline{B}}$ and $\overline{\overline{M}}_T$ were defined in Eq. (26).

$$\left.\begin{aligned}&\overline{\overline{A}}=\begin{bmatrix}0&-n(\overline{Q_{23}}^*+\overline{Q_{44}}^*)&-n(\overline{Q_{36}}^*+\overline{Q_{45}}^*)&\overline{Q_{33}}^*&0&0\\n(\overline{Q_{44}}^*+\overline{Q_{23}}^*)&0&\overline{Q_{45}}^*&0&\overline{Q_{44}}^*&\overline{Q_{45}}^*\\(\overline{Q_{36}}^*+\overline{Q_{45}}^*)n&-\overline{Q_{45}}^*&0&0&\overline{Q_{45}}^*&\overline{Q_{55}}^*\\1&0&0&0&0&0\\0&1&0&0&0&0\\0&0&1&0&0&0\end{bmatrix}\\&\overline{\overline{B}}=\begin{bmatrix}(\overline{Q_{22}}^*+n^2\overline{Q_{44}}^*)&-n(\overline{Q_{22}}^*+\overline{Q_{44}}^*)&-n\overline{Q_{26}}^*&0&0&0\\-(\overline{Q_{44}}^*+\overline{Q_{22}}^*)n&(\overline{Q_{44}}^*+\overline{Q_{22}}^*n^2)&\overline{Q_{26}}^*n^2&0&0&0\\-\overline{Q_{26}}^*n&\overline{Q_{26}}^*n^2&\overline{Q_{66}}^*n^2&0&0&0\\0&0&0&1&0&0\\0&0&0&0&1&0\\0&0&0&0&0&1\end{bmatrix}\\&\overline{\overline{M}}_T=\rho^2\begin{bmatrix}\overline{\beta}_r\overline{T}\rho\tau n_{,\rho}+(\overline{\beta}_r-\overline{\beta}_\theta)\rho^{-1}\overline{T}\rho\tau n\\n\overline{\beta}_\theta\rho^{-1}\overline{T}\rho\tau n\\n\overline{\beta}_{\theta z}\rho^{-1}\overline{T}\rho\tau n\\0\\0\\0\end{bmatrix}\end{aligned}\right\} \tag{26}$$

Finally, the solution of (23) can be presented in the following form

$$\overline{\overline{U_n}} = \begin{bmatrix} U_{rn} \\ U_{\theta n} \\ U_{zn} \\ U'_{rn} \\ U'_{\theta n} \\ U'_{zn} \end{bmatrix} = \overline{\overline{V}} \left(\overline{\overline{e}} \begin{bmatrix} c_1 \\ c_2 \\ c_3 \\ c_4 \\ c_5 \\ c_6 \end{bmatrix} + \int_{\rho}^{\bar{a}} \overline{\overline{e}} \overline{\overline{V}}^{-1} \begin{bmatrix} \rho \bar{\beta}_r \bar{T} \rho\tau n_{,\rho} + (\bar{\beta}_r - \bar{\beta}_\theta) \bar{T} \rho\tau n \\ n \bar{\beta}_\theta \bar{T} \rho\tau n \\ n \bar{\beta}_{\theta z} \bar{T} \rho\tau n \\ 0 \\ 0 \\ 0 \end{bmatrix} d\rho \right) \tag{27}$$

where the matrix $\overline{\overline{e}}$ is diagonal matrix and the diagonal kith element and can be displayed as $\overline{\overline{e}}_k = e^{(-\gamma_{nk} \ln \rho)}$. Also, γ_{nk}, is the eigenvalue and $\overline{\overline{V}}$, is the matrix of eigenvectors of $\overline{\overline{A}}^{-1}\overline{\overline{B}}$.

In the above equation, the unknown parameters c_1, ..., c_6 are found from the boundary conditions Eq. (17) for each layer. Noteworthy is that adding of mechanical loading in boundary conditions, only changes the constant parameter c_i. Substituting displacement from Eq. (27) into strain-displacement equations, Eq. (16), and using stress-strain equation, Eq. (15), the stresses in each layer are obtained as

$$\begin{bmatrix} \bar{\sigma}_z \\ \bar{\sigma}_\theta \\ \bar{\sigma}_r \\ \bar{\sigma}_{r\theta} \\ \bar{\sigma}_{rz} \\ \bar{\sigma}_{\theta z} \end{bmatrix} = \sum_{n=1}^{\infty} \overline{Q}^* \left(\begin{bmatrix} -\bar{T}_{\rho\tau n} \alpha_z \\ \dfrac{\overline{\overline{U_n}}(4)}{\rho} - \bar{T}_{\rho\tau n} \alpha_\theta \\ \dfrac{1}{\rho}\left(\overline{\overline{U_n}}(1) - n\overline{\overline{U_n}}(2) \right) - \bar{T}_{\rho\tau n} \alpha_r \\ 0 \\ 0 \\ -\dfrac{n}{\rho}\overline{\overline{U_n}}(3) - \bar{T}_{\rho\tau n} \alpha_{z\theta} \end{bmatrix} \times \right.$$
$$\times (A_n \sin(n\theta) + B_n \cos(n\theta)) + (A_n \cos(n\theta) - B_n \sin(n\theta)) \times$$
$$\left. \times \begin{bmatrix} 0 \\ 0 \\ 0 \\ \dfrac{\overline{\overline{U_n}}(5) + n\overline{\overline{U_n}}(1) - \overline{\overline{U_n}}(2)}{\rho} \\ \dfrac{\overline{\overline{U_n}}(6)}{\rho} \\ 0 \end{bmatrix} \right) \tag{28}$$

where $\overline{\overline{U_n}}(i)$ is ith member of the matrix $\overline{\overline{U_n}}$.

3. Numerical results

For validation of the proposed solution, the results were compared with the stress function method solution in isotropic case (in reference [9]) which is a special type of our solution. It is seen that the results are in close agreement and the average error in each case is less than 0.5%. Further two-layered pipe with different boundary contions are investigated. The temperature and stresses in all figures of this paper are on the maximum value in the angular direction. According to Eq. (28) and thermal boundary conditions in these cases, the maximum peripheral angles, θ, for the temperature, $\bar{\sigma}_{r\theta}$ and $\bar{\sigma}_{rz}$ is 90° and for other stresses is 0°. Because of using series method, an oscillating zone in the outer boundary can be seen in the most of the figures.

To illustrate the foregoing analyses, a typical composite pipe which composed of E-Glass/Epoxy with the material properties as stated in Table 1 is considered.

Table 1
Material properties for CNG pressure Vessels [10]

Properties	Value
E_{11}, kg/mm^2	5483.946
E_{22}, kg/mm^2	1827.982
E_{33}, kg/mm^2	1927.982
ν_{12}, ν_{13}	0.25
G_{12}, kg/mm^2	913.991

The thermal conductivity and thermal expansion coefficients are considered as [2]

$$\left. \begin{aligned} k_L &= 41.1\times10^{-6}\,\frac{\mathrm{m}^2}{\mathrm{s}},\ k_T = 29.5\times10^{-6}\,\frac{\mathrm{m}^2}{\mathrm{s}} \\ \alpha_L &= 7.6\times10^{-6}\,\frac{1}{\mathrm{K}},\ \alpha_T = 14.0\times10^{-6}\,\frac{1}{\mathrm{K}} \end{aligned} \right\} \tag{29}$$

It is assumed that each layer consists of the same orthotropic material. A 2-layered antisymmetric angle-ply laminated hollow cylindrical with the fibber orientation ($\phi/-\phi$) with the same thickness is assumed. The inner and outer dimensionless radii are taken as 0.9 and 1 respectively. Following cases are investigated

1 - $\dfrac{\bar{T}(1,\theta,\tau) = sin(\theta)}{\bar{T}(\bar{a},\theta,\tau) = 0}$, $\phi = \pm 85^\circ$

2 - $\dfrac{\bar{T}(1,\theta,\tau) = sin(\theta)sin(2\pi\tau)}{\bar{T}(\bar{a},\theta,\tau) = 0}$, $\phi = \pm 85^\circ$

3 - $\dfrac{\bar{T}(1,\theta,\tau) = sin(\theta)}{\bar{T}(\bar{a},\theta,\tau) = 0}$, $\phi = \pm 55^\circ$

For the sake of brevity, the results of case 2 and 3 are not drawn and only the maximum stresses of these conditions are compared with case 1.

3.1. Results for case 1

Fig. 2 shows that the temperature distribution changes quickly in the time from $\tau = K_0 t / b^2 =$

$= 0.001 - 0.003$ and reaches finally to the steady state on $\tau = 0.005$.

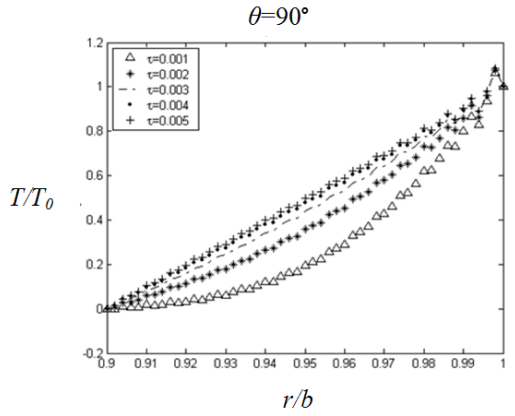

Fig. 2 Time-dependent temperature distribution versus the dimensionless radial distance (case 1)

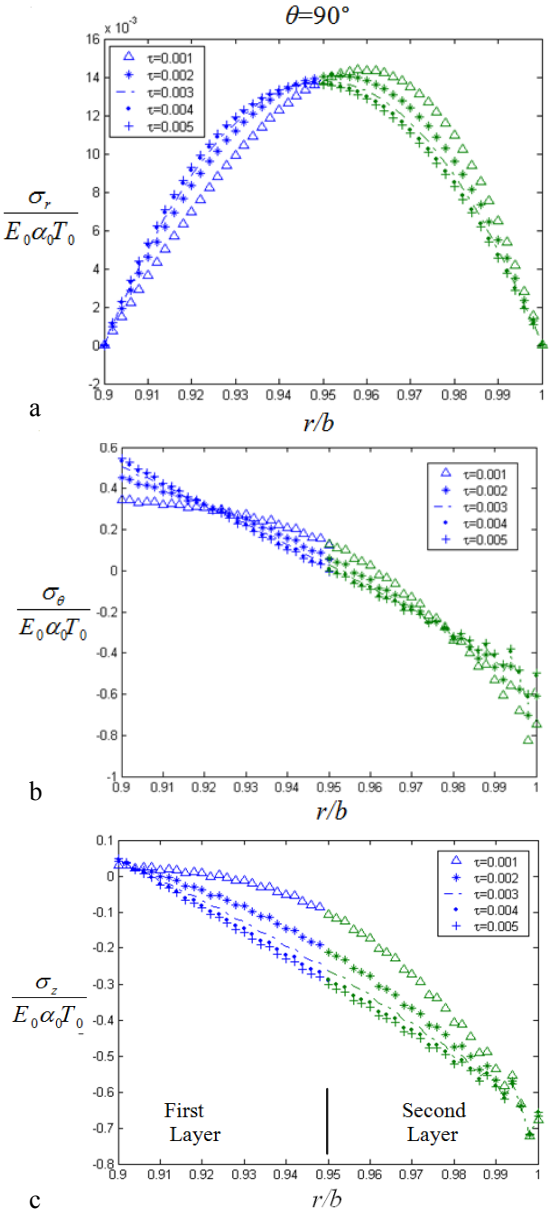

Fig. 3 Time-dependent distribution of the dimensionless a) radial stress, b) hoop stress, c) longitudinal stress versus the dimensionless radial distance

The distributions of the radial stress, hoop stress and longitudinal stress across the thickness of the cylinder at different instants of time were shown in Fig. 3.The high values of hoop and longitudinal stresses in the external boundary of the cylinder can be noticed. The maximum value of radial stress changes with time duration and its position approaches to the centre of cylinder.

This stress is small in comparison with the hoop and longitudinal stresses, but has a significant effect on the destruction of layers [2]. In addition, the maximum values of normal stresses decrease as the time proceeds.

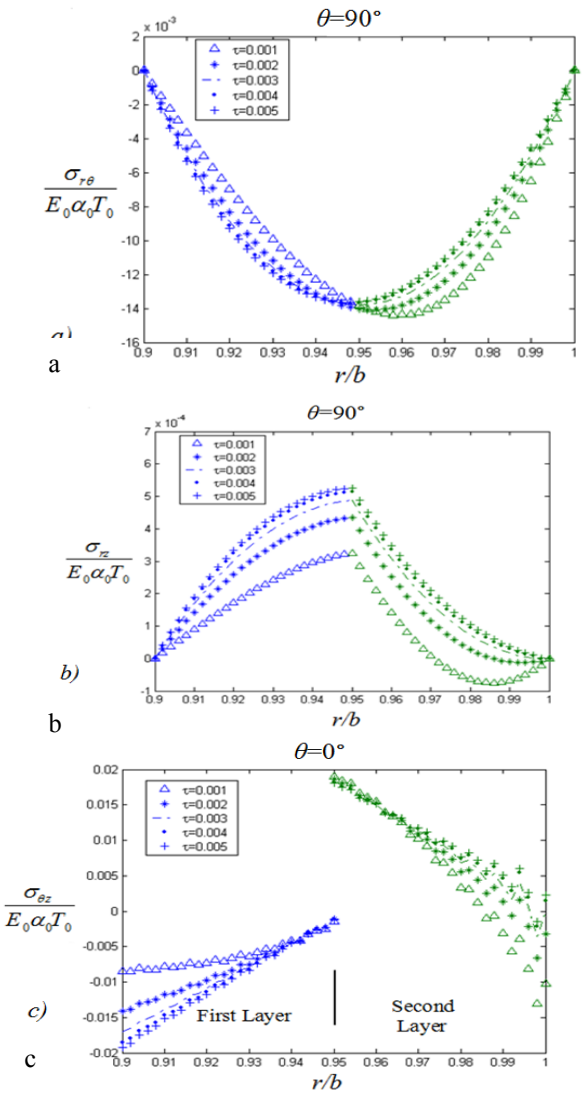

Fig. 4 Time-dependent distribution of the a) $\bar{\sigma}_{r\theta}$, b) $\bar{\sigma}_{rz}$, c) $\bar{\sigma}_{z\theta}$ versus the dimensionless radial distance

The variation of the shearing stresses indicated in the Fig. 4. It can be noticed that the shearing stresses $\sigma_{rz}, \sigma_{z\theta}$ and $\sigma_{r\theta}$ show the maximum value on the interface of layers.

The shearing stress $\bar{\sigma}_{r\theta}$ shows the maximum value near $\rho = 0.96$ in a transient state. The value of the shearing stress $\bar{\sigma}_{rz}$, rises as the time proceeds and has a maximum value in the steady state.

The maximum values of $\bar{\sigma}_{z\theta}$ are in the interface of layers which does not change with time. The maximum

of stresses for different boundary conditions and angles are compared and shown in Table 2.

Table 2

Maximum absolute stresses for different boundary conditions

Case:	1 (Sudden)	2 (Sinusoidal)	3 (Sudden)
Orientation:	$\phi = \pm 85^{\circ}$	$\phi = \pm 85^{\circ}$	$\phi = \pm 55^{\circ}$
$\overline{\sigma}_{zz}$	0.7	0.7	0.8
$\overline{\sigma}_{\theta\theta}$	0.8254	0.58	0.70
$\overline{\sigma}_{rr}$	0.014	0.0136	0.0114
$\overline{\sigma}_{z\theta}$	0.01923	0.0199	0.0986
$\overline{\sigma}_{rz}$	0.00053	0.00053	0.0023
$\overline{\sigma}_{r\theta}$	0.014	0.0136	0.0114

The high value of longitudinal stress in sinusoidal loading compare to sudden loading can be noticed. In addition, the maximum stress is on the hoop stress for $\phi = \pm 85^{\circ}$ for sudden loading. Increasing in angle of orientation result in increasing all stresses except of $\overline{\sigma}_{z}$ and $\overline{\sigma}_{rz}$.

4. Conclusion

The results of numerical analyses in summary can be classified as follows:

1. by increasing angle of orientation; the amount of stress discontinuity in layer interface reduces;
2. the most discontinuity in the stresses is seen in $\overline{\sigma}_{\theta z}$;
3. the shearing stresses $\overline{\sigma}_{rz}, \overline{\sigma}_{z\theta}$ and $\overline{\sigma}_{r\theta}$ show the maximum value on the interface of the layers;
4. in an anisotropic cylinder for two dimensional temperature fields, the strain in the axial direction is available and varies with time, but in the isotropic cylinder this strain is zero;
5. the longitudinal stress in sinusoidal loading comparing to a sudden loading has great value;
6. the increasing in the angle of orientation in sudden loading, results in all stresses increasing. Further for the sudden loading, the maximum stress is the hoop stress;
7. in the sinusoidal loading the hoop stress is less than the sudden loading and the maximum stress is longitudinal stress.

References

1. **Lee, Z.Y.** 2005. Hybrid numerical method applied to 3-D multilayered hollow cylinder with periodic loading conditions, Appl. Math. Comput. 166: 95-117.
2. **Ootao, Y.; Tanigawa, Y.** 2001. Transient thermal stresses of angle-ply laminated cylindrical panel, Composite Structures 55: 95-103.
3. **Shahani, A.R.; Nabavi, S.M.** 2007. Analytical solution of the quasi-static thermo elasticity problem in a pressurized thick-walled cylinder subjected to transient thermal loading, Applied Mathematical Modeling 31: 1807-1818.
4. **Radu, V.; Taylor, N.; Paffumi, E.** 2008. Development of new analytical solutions for elastic thermal stress components in a hollow cylinder under sinusoidal transient thermal loading, International Journal of Pressure Vessels and Piping 85: 885-893.
5. **Hocine, A.; Bezazi, A.; Boubakar, L**.; **Kondratas, A.** 2006. Multi layer tubular composite reinforced by a liner: behaviourunder thermo mechanical loading simulation, Mechanika 2(58): 17-23.
6. **Zamani Nejad, M.; Rahimi, G.H.; Ghannad, M.** 2009. Set of field equations for thick shell of revolution made of functionally graded materials in curvilinear coordinate system, Mechanika 3(77): 18-26.
7. **Bakaiyan, H.; Hosseini, H.; Ameri, E.** 2009. Analyses of multi-layered filament-wound composite pipes under combined internal pressure and thermomechanical loading with thermal variations, Composite Structures 88: 532-541.
8. **Mridula, G.; Alka, R.; Kalla, S.L.** 2007. On a generalized finite Hankel transform, Applied Mathematics and Computation 190: 705-711.
9. **Hetnarski, R.; Eslami, M.** 2008. Thermal Stresses Advanced Theory and Application. Springer.
10. **Choi, J.; Kim, C.; Jung, S.Y.** 2004. Development of an automated design system of a CNG composite vessel using a steel liner manufactured using the DDI process, Int J Adv Manuf Technol.24: 781-788.

M.A. Ehteram, M. Sadighi, H. Basirat Tabrizi

LAMINUOTO TUŠČIAVIDURIO CILINDRO APKROVIMO NESTACIONARIA NEVIENALYTE ŠILUMINE APKROVA ANALITINIS SKAIČIAVIMAS

R e z i u m ė

Šiluminiams įtempiams tiksliai apskaičiuoti keičiantis temperatūrai ir esant pastoviai apskritiminei apkrovai, naudojamos baigtinės Henkelio ir Furje transformacijos. Atlikti dviejų sluoksnių tuščiavidurio cilindro su skirtingo pluošto orientacijos kampais skaičiavimai dinamiškai ir cikliškai keičiantis temperatūrai. Rezultatai rodo, kad esant dinaminei apkrovai ir didėjant orientacijos kampui, visi įtempiai didėja, palyginant su statinės apkrovos sukeltais įtempiais. Be to, esant dinaminei apkrovai, didžiausi yra žiediniai įtempiai. Esant ciklinei apkrovai, žiediniai įtempiai yra mažesni, negu esant dinaminei apkrovai. Šiuo atveju didžiausi yra išilginiai įtempiai. Didžiausi tangentiniai įtempiai susidaro sluoksnių sandūroje ir nepriklauso nuo apkrovimo sąlygų.

M. A. Ehteram, M. Sadighi, H. Basirat Tabrizi

ANALYTICAL SOLUTION FOR THERMAL STRESSES OF LAMINATED HOLLOW CYLINDERS UNDER TRANSIENT NONUNIFORM THERMAL LOADING

S u m m a r y

An analytical solution for the temperature change and thermal stresses for the circumferential transient loading are obtained using finite Hankel and Fourier transform. Numerical calculations are carried out for a two-layered

angle-ply hollow cylinder in the different orientation angles with sudden and periodic temperature change with time. The results indicate that the increasing in the angle of orientation in sudden loading, results in all stresses increasing comparing to steady state condition. Further for the sudden loading, the maximum stress is the hoop stress. In a periodic loading the hoop stress is less than the sudden loading and the maximum stress is longitudinal stress. The maximum of shear stresses occur in interface of layers and is constant with time for all conditions.

М.А. Ехтерам, М. Садигхи, Х. Басират Табризи

АНАЛИТИЧЕСКОЕ РЕШЕНИЕ ЛАМИНИРОВАННОГО ПУСТОТЕЛОГО ЦИЛИНДРА ПРИ НЕСТАЦИОНАРНОЙ НЕОДНОРОДНОЙ ТЕПЛОВОЙ НАГРУЗКЕ

Р е з ю м е

Точное решение тепловых напряжений при изменении температуры и постоянной окружной нагрузке получено при использовании конечных трансформаций Хенкеля и Фурье. Числовые решения получены для двухслойного пустотелого цилиндра с учетом различной ориентации волокон при динамическом и циклическом изменении температуры во времени. Результаты показывают, что при динамической тепловой нагрузке и увеличении угла ориентации, все напряжения возрастают по сравнению со статической нагрузкой. Кроме того, при динамической нагрузке максимальными являются окружные напряжения. При циклической нагрузке окружные напряжения меньше по сравнению с динамической нагрузкой и в этом случае максимальными являются осевые напряжения. Максимальные тангенциальные напряжения действуют на стыке слоев, являются постоянными при изменении условий нагрузки.

Received August 18, 2010
Accepted January 17, 2011